

Resonant and preresonant Raman scattering in C_{60} and $K_6 C_{60}$ films

V. N. Denisov and B. N. Mavrin

Institute of Spectroscopy, Russian Academy of Sciences

G. Ruani, R. Zamboni, and C. Taliani

Istituto di Spettroscopia Molecolare, CNR, Bologna, Italy

(Submitted 5 February 1992)

Zh. Eksp. Teor. Fiz. **102**, 300–312 (July 1992)

The vibrations of the C_{60} molecule and of the C_{60} , $K_3 C_{60}$, and $K_6 C_{60}$ crystals are classified by group theory. In crystals, the intramolecular H_g vibrations should split into doublets which are active in Raman scattering. In addition, bands corresponding to translations of potassium atoms and to reorientations of C_{60} molecules should be seen in the Raman spectra and the IR absorption spectra of $K_3 C_{60}$ and $K_6 C_{60}$. Raman spectra of C_{60} and $K_6 C_{60}$ films were recorded during excitation at the wavelengths $\lambda_i = 488, 514.5, 647.1,$ and 1064 nm. The $K_6 C_{60}$ spectra reveal a splitting of the H_g modes into doublets. These spectra also have some low-frequency bands, which are assigned to translations of potassium atoms and to reorientations of molecules. In C_{60} , the intensity of the A_g modes is determined exclusively by the Franck–Condon factor, while that of the H_g modes is determined exclusively by the Herzberg–Teller interaction. The changes expected in the internuclear distances in the excited state of C_{60} are similar in shape to the normal A_g vibration at 1468 cm^{-1} . The A_g modes have an anomalously low intensity in $K_6 C_{60}$ in the case of excitation at $\lambda_i = 1064$ nm. This effect is attributed to an interference of the contributions from different electronic states. The second-order Raman spectra are discussed.

1. INTRODUCTION

The discovery¹ of superconductivity in the fullerene C_{60} doped with an alkali metal ($M = K, Rb,$ or Cs) has heightened interest in the spectroscopic and other physical properties of the new class of high- T_c superconductors with the general formula $M_x C_{60}$. It turns out that the superconductivity is observed only at $x \approx 3$, and T_c can reach 33 K (Ref. 2). At the maximum doping level ($x \approx 6$), the superconductivity disappears.

For the fullerene C_{60} , we now have Raman scattering spectra,^{3–8} IR absorption spectra,^{9,13} neutron-scattering spectra,¹⁴ electron-absorption spectra,¹⁰ and triplet-triplet absorption spectra.^{15,16} The neutron scattering spectra¹⁷ and the Raman spectra^{4,8} have also been studied for $K_3 C_{60}$; Raman spectra have been measured for $M_6 C_{60}$ (Refs. 4, 6, and 8). All the Raman-active ($2A_g + 8H_g$) and IR-active ($4F_{1u}$) intramolecular vibrations of the C_{60} molecule have been observed in the vibrational spectra. Furthermore, the Raman spectra of $K_x C_{60}$ have a continuum, which has been attributed to a Raman scattering by low-energy electronic excitations and also to a Fano resonance of a low-frequency intramolecular vibration with this continuum.⁸ As the number of alkali metal atoms increases, the high-frequency tangential mode A_g softens significantly (Refs. 4 and 6). This softening has been attributed to a lengthening of the C–C bond as the result of charge transfer.

The interpretation of the vibration spectra of C_{60} and $M_x C_{60}$ has so far been based on the isolated C_{60} molecule. Although the intermolecular interaction is expected to be much weaker than the intramolecular interaction in molecular crystals such as the solid fullerenes, it is worthwhile to determine how the crystal field affects the vibrational properties of these crystals. There is particular interest in the

observation of intermolecular modes (translations of alkali metal atoms and translations and reorientations of C_{60} molecules), since they may be responsible for the low values of T_c (Ref. 18) in the phonon theories for the superconductivity of $M_3 C_{60}$ (Ref. 19). We have accordingly undertaken an effort to observe the low-frequency intermolecular modes in the Raman spectra of C_{60} and $K_6 C_{60}$ and also determine how the crystal field affects the spectra of the intramolecular vibrations.

The electronic spectra of C_{60} and $M_x C_{60}$ have received less study, but electronic absorption spectra of C_{60} (Ref. 10) and photoemission spectra of C_{60} and $K_x C_{60}$ (Ref. 20) have been reported. The electronic structure of C_{60} has been calculated.^{21,22} It has been found that the lowest allowed electronic transition in C_{60} has a wavelength shorter than 350 nm (Refs. 10, 21, 22). In addition, some faint absorption bands have been observed in the visible part of the spectrum¹⁰ and have been assigned to symmetry-forbidden electronic transitions in C_{60} (Ref. 15).

According to photoemission data,²⁰ the energy distance between the highest occupied molecular orbital (HOMO) and the lowest unoccupied molecular orbital (LUMO) decreases from 4 eV in a C_{60} film to 1.6 eV when C_{60} is completely saturated with potassium atoms. Such a striking change in the energy gap should have an important effect on the Raman spectra, for when the spectra are excited in the usual way, by light in the visible region, the energy of the exciting photons is much smaller than (in the case of C_{60}) or greater than (in the case of $K_6 C_{60}$) the energy gap. In the present study we have investigated the resonant excitation profiles of the Raman scattering in C_{60} and $K_6 C_{60}$ in the region 1.16 – 2.54 eV in order to identify the mechanisms for the intensification of the resonant Raman scattering.

Let us briefly outline the paper. In Sec. 2 we present

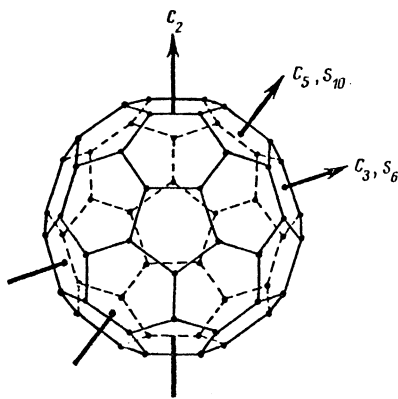


FIG. 1. The C_{60} molecule and some of the symmetry axes.

structural data and the results of a group-theory analysis of the vibrations in C_{60} and $K_x C_{60}$. The experimental Raman spectra are discussed in Sec. 3. Here the experimental procedure is described (Subsec. 3.1), the intramolecular and intermolecular vibrational spectra are reported (Subsec. 3.2), the mechanisms for Raman scattering in C_{60} and for resonant Raman scattering in $K_6 C_{60}$ are studied (Subsecs. 3.3 and 3.4), and the second-order Raman spectra are discussed (Subsec. 3.5).

2. GROUP-THEORY ANALYSIS

2.1. Structural data

The C_{60} molecule has icosahedral symmetry I_h . All 60 carbon atoms lie on the surface of a sphere about 7 \AA in diameter, forming 12 pentagons and 20 hexagons (Fig. 1). The carbon atoms occupy sites characterized by the symmetry point group C_5 .

Table I shows structural parameters of the crystals. While the C_{60} and $K_3 C_{60}$ crystals have an *fcc* lattice, $K_6 C_{60}$ has a *bcc* lattice.

At room temperature, the molecules in a C_{60} crystal are rotating freely.²⁶ As the temperature is lowered (below 260 K), a transition occurs from an isotropic rotational diffusion to hops of molecules between symmetry-equivalent orientations.²⁷ According to other data,²⁸ the molecular reorientations cease as the temperature is lowered.

In the $K_3 C_{60}$ crystal, the orientations of the C_{60} molecules are statistically disordered in two dimensions, in such a way that the *z* axis of the crystal always passes through the

midpoint of the bond between two neighboring hexagons and the center of the molecule [along the C_2 axis of the molecule (Fig. 1)]. The *x* axis (like the *y* axis) of the crystal is either parallel to or perpendicular to this bond. In the $K_6 C_{60}$ crystal, the molecules do not rotate; their orientation is the same as in $K_3 C_{60}$, except that it is fixed.

2.2. Intramolecular vibrations in the isolated C_{60} molecule and in the C_{60} , $K_3 C_{60}$, and $K_6 C_{60}$ crystals

Knowing the symmetry group of the free C_{60} molecule and the positional symmetry group of the carbon atoms, we can easily determine the vibrational representation for the isolated C_{60} molecule by the method of positional symmetry:²⁹

$$\Gamma = 2A_g + 4F_{1g} + 4F_{2g} + 6G_g + 8H_g + A_u + 5F_{1u} + 5F_{2u} + 6G_u + 7H_u. \quad (1)$$

In this representation, one F_{1u} vibration and one F_{1g} vibration correspond to the translation and rotation, respectively, of the molecule as a whole. The other vibrations are intramolecular; of them, $2A_g + 8H_g$ are Raman-active, while $4F_{1u}$ are IR-active. The same vibrational representation was derived previously, by a more complicated method, involving projection operators of icosahedral symmetry.³⁰

The primitive cell of the C_{60} , $K_3 C_{60}$, and $K_6 C_{60}$ crystals contains only one C_{60} molecule (Table I). We would thus not expect a dynamic interaction of the molecules, so we would not expect a Davydov splitting of the intramolecular vibrations. However, the positional symmetry group of the molecules in the crystals (Table I) is lower than the symmetry of the isolated molecule, I_h . We would thus expect the degeneracy of certain degenerate vibrations to be lowered by a static crystal field (a Bethe splitting). This effect can be analyzed by means of the correlation of irreducible representations of the point groups of the crystal and the positions.

It follows from this analysis that the Raman-active, quintuply degenerate H_g vibrations should split into Raman-active doublets ($E_g + F_{2g}$ in C_{60} and $K_3 C_{60}$; $E_g + F_g$ in $K_6 C_{60}$). The nondegenerate Raman-active A_g vibrations and the IR-active F_{1u} modes do not split. The crystal field should thus cause the eight bands of symmetry H_g in the Raman spectra to be replaced by eight doublets, whose components differ in symmetry. The distance between the components of a doublet can serve as a measure of the strength of the crystal field.

TABLE I. Structural parameters of the fullerene crystals.

Crystal	Symmetry space group	z_u	z_p	a , A	Positional symmetry group		Source
					C_{60} molecules	K atoms	
C_{60}	$Fm\bar{3}m (O_h^5)$	4	1	14,11	O_h	—	[23]
$K_3 C_{60}$	$Fm\bar{3}m (O_h^5)$	4	1	14,24	O_h	O_h, T_d^*	[24]
$K_6 C_{60}$	$Ih\bar{3} (T_h^5)$	2	1	11,39	T_h	C_{2v}	[25]

Notation. Here z_u and z_p are the number of formula units in the unit cell and the primitive cell, respectively, and a is the lattice constant.

*Of the 12 potassium atoms in the unit cell in the $K_3 C_{60}$ crystal, four are in octahedral O_h sites, and eight are in tetrahedral T_d sites.

2.3. Intermolecular vibrations of C_{60} molecules; translational modes of potassium in C_{60} , K_3C_{60} , and K_6C_{60} crystals

The vibrations in the C_{60} molecular crystal can be classified as either intramolecular vibrations (which we discussed above) or intermolecular vibrations, consisting of translations and reorientations of C_{60} molecules with respect to each other. In the K_3C_{60} and K_6C_{60} crystals, translational motions of the potassium atoms are added to the intermolecular vibrations. Intermolecular vibrations can again be analyzed by the positional-symmetry method.²⁹ As a result, the vibrational representations of the intermolecular modes are found to be

$$\begin{aligned}\Gamma_0 &= F_{1g}^M + F_{1u}^M, \\ \Gamma_3 &= F_{1g}^M + F_{2g}^K + 3F_{1u}, \\ \Gamma_6 &= A_g^K + E_g^K + 2F_g^K + F_g^M + 4F_u\end{aligned}\quad (2)$$

for the C_{60} , K_3C_{60} , and K_6C_{60} crystals, respectively. The index K specifies a mode in which only potassium atoms participate; the index M specifies C_{60} molecules exclusively; and both potassium atoms and C_{60} molecules participate where there is no index. These representations include one triply degenerate acoustic mode (F_{1u} in C_{60} and K_3C_{60} ; F_u in K_6C_{60}).

Accordingly, only the one mode F_{1g} (corresponding to a reorientation of the C_{60} molecules) is an optical mode in the C_{60} crystal, but this mode is Raman- and IR-inactive. Active in the Raman spectra are one translational mode of potassium (F_{2g}^K) in K_3C_{60} , four translation modes of potassium ($A_g^K + E_g^K + 2F_g^K$), and one orientational mode of the C_{60} molecules (F_g^M) in K_6C_{60} . Two (three) translational modes are active in the IR spectra of K_3C_{60} (K_6C_{60}). These modes involve both potassium atoms and C_{60} molecules.

3. EXPERIMENTAL RESULTS AND DISCUSSION

3.1. Experimental procedure

The C_{60} and K_6C_{60} films, $\approx 1 \mu\text{m}$ thick, were deposited on substrates of crystalline silicon or glass by the standard technique.⁹ The K_6C_{60} film was sealed-off in an evacuated glass tube.

The Raman spectra excited at a wavelength $\lambda_i = 1064$ nm were analyzed on a Bruker IFS 88 Fourier spectrometer.⁸ The spectra excited by the lines from the argon-krypton laser (488–647.1 nm) were recorded by a multichannel spectrometer with a triple reduction of spectral width.³¹ The spectral resolution was $\approx 4 \text{ cm}^{-1}$. The laser power did not exceed 10 mW. The power density reached 100 W/cm^2 . The Raman scattering intensity was calibrated on the basis of Raman scattering lines of calcite. The exciting laser beam was incident at a grazing angle.

In the case of the C_{60} film, which was exposed to the atmosphere and thus to the effects of oxygen, the spectra were recorded after 10–15 min of illumination with the laser beam (at 514.5 nm), in order to reach equilibrium conditions for the sample.⁷

3.2. Raman spectra of intramolecular and intermolecular vibrations

3.2.1. C_{60} . Figure 2 shows Raman spectra of a C_{60} film excited at various wavelengths. At $\lambda_i = 488$ nm we see ten

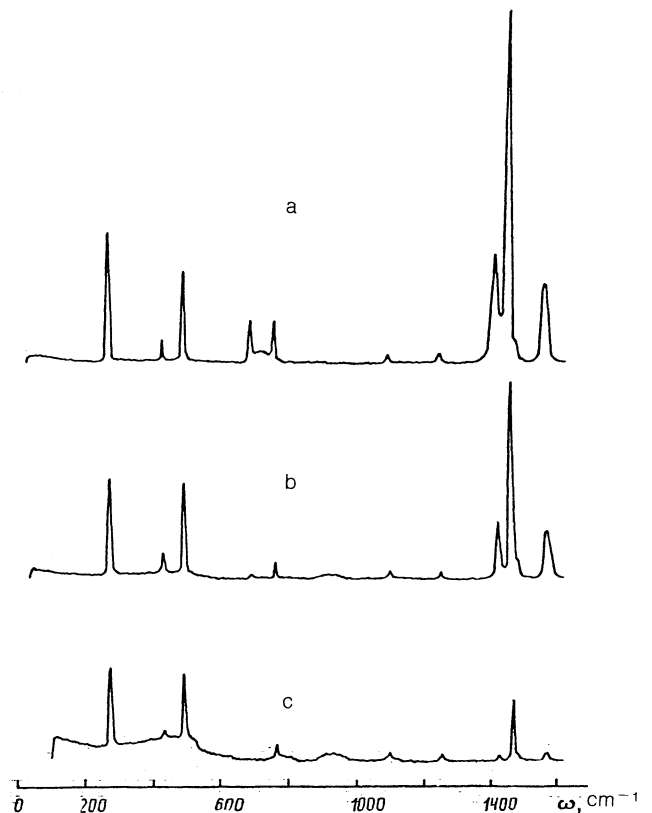


FIG. 2. Raman spectra of a C_{60} film. a—Excitation at the wavelength $\lambda_i = 488$, b—647.1, and c—1064 nm.

bands in the spectrum, two of which (496 and 1468 cm^{-1}) correspond to A_g vibrations,⁶ while the eight others correspond to quintuply degenerate H_g vibrations. This result corresponds to the results of the group-theory analysis [see (1)]. The frequencies in the Raman spectra of the C_{60} and K_6C_{60} films are shown in Table II. Their identification is also shown here, and the experimental results are compared with the theoretical results. The shapes of the normal vibrational modes are known from calculations.^{22,30} In particular, the band at 496 cm^{-1} corresponds to completely symmetrical radial breathing vibrations of all carbon atoms, and the band at 1468 cm^{-1} corresponds to a tangential motion of atoms in the course of which the carbon atoms in the pentagons undergo breathing vibrations along the tangent to the surface of the sphere. The shapes of the low-frequency H_g vibrations also correspond to radial displacements of the atoms, while those of the high-frequency vibrations correspond to tangential displacements. In particular, the mode at 271 cm^{-1} corresponds to a vibration which deforms the spherical molecule into the shape of a rugby ball.

The H_g band at 271 cm^{-1} has a significant low-frequency asymmetry, which can be interpreted as an overlap of components. The other H_g bands do not exhibit a splitting. If there is a splitting here, it is smaller than the width of the bands. A small splitting is evidence of a weak crystal field. This situation may be a consequence of a free rotation of the molecules and also of a weak van der Waals intermolecular interaction, which determines the strength of this field.

In accordance with the group-theory predictions [see (2)], we were unable to find low-frequency bands ($< 270 \text{ cm}^{-1}$) in the region $\omega \geq 30 \text{ cm}^{-1}$. Such bands might

TABLE II. Frequencies of the bands (in reciprocal centimeters) in the Raman spectra of C_{60} and K_6C_{60} crystals.

C_{60}			K_6C_{60}	C_{60}			K_6C_{60}
Theor ²²	Assignment	Expt.	Expt.	Theor ²²	Assignment	Expt.	Expt.
258	H_g	271	{ 267 * 280 419	1154	H_g	1100	{ 1091 1118
440	H_g	431	{ 426 500	1265	H_g	1250	1234
513	A_g	496	{ 655	1465	H_g	1424	1386
691	H_g	709	{ 675	1442	A_g	1468	1430
801	H_g	772	{ 726 760	1644	H_g	1574	{ 1473 1480

*In addition to the frequencies specified here, the spectrum has bands at 30, 40(?), 48, 72, and 105 cm^{-1} (see the text proper).

have been attributed to intermolecular modes in the C_{60} film.

3.2.2. K_6C_{60} . The Raman spectra of the K_6C_{60} film (Figs. 3 and 4; Table II) are quite different from the spectrum of the C_{60} film (Fig. 2).

First, several low-frequency bands appear in the K_6C_{60} spectrum: at 33, 48, 72, and 105 cm^{-1} . Of these bands, the first two can be seen only in the case of excitation at $\lambda_i = 647.1$ nm, in which case the parasitically scattered light is suppressed relatively effectively in our spectrometer. In addition to these bands, the spectra reveal another, very weak band near 40 cm^{-1} , which is seen as a slight knee on

the intense band at 33 cm^{-1} (Fig. 4). These bands can naturally be attributed to intermolecular modes, since we would expect five intermolecular bands ($A_g + E_g + 3F_g$) in this frequency region according to the group-theory predictions [see (2)]. Of these five bands, four ($A_g + E_g + 2F_g$) should correspond to translational motions of potassium atoms, and one (F_g) should correspond to orientational vibrations of the C_{60} molecules with respect to each other.

We have a few comments regarding the identification of the bands. We would expect the frequencies of the translational vibrations of the light potassium atoms to be higher than the frequencies of the orientational vibrations of the large C_{60} molecules.³² In particular, the band at 105 cm^{-1} can thus be attributed to translational vibrations of potassium atoms. On the other hand, the intensity of this band

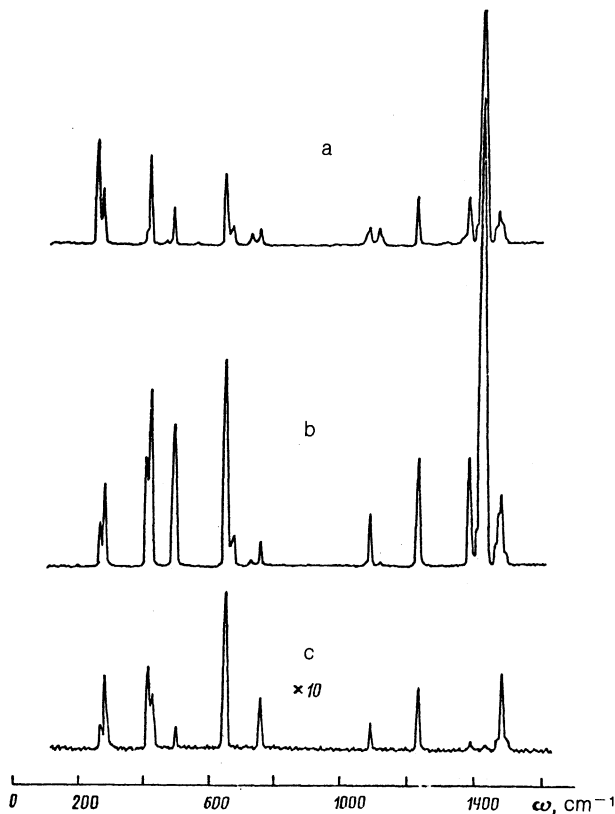


FIG. 3. Raman spectra of intramolecular vibrations of a K_6C_{60} film. a—Excitation at $\lambda_i = 488$, b—647.1, and c—1064 nm.

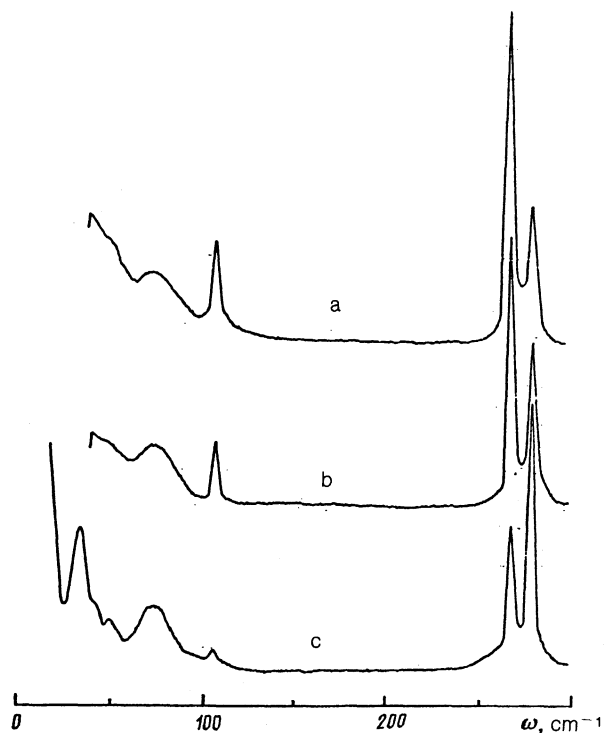


FIG. 4. Raman spectra of the intermolecular vibrations of a K_6C_{60} film. a—Excitation at $\lambda_i = 488$, b—514.5, and c—647.1 nm.

increases sharply with decreasing excitation wavelength (Fig. 4), i.e., as we approach an allowed electronic transition. Properties of this type are usually exhibited by a Franck–Condon component of the Raman cross section; such a component is important only for completely symmetric vibrations.³³ On this basis we assume that the band at 105 cm⁻¹ can be attributed to A_g vibrations. The preferred assignment of the band at 33 cm⁻¹ to orientational vibrations is based on the circumstance that orientational vibrations are usually intense in Raman spectra.³²

The comparatively large width of the 72-cm⁻¹ band among the low-frequency bands is interesting. This width may be a consequence of a strong interaction of this phonon with charge carriers. If so, we could regard this low-frequency band as one of the ones responsible for the low value of T_c in the superconducting system $M_x C_{60}$ (Ref. 18).

According to the group-theory analysis, the quintuply degenerate intramolecular vibrations H_g should split into doublets $E_g + F_g$ in the Raman spectra of $K_6 C_{60}$. Indeed, we see such doublets, at least for six bands (Table II) with splittings ranging from 7 to 34 cm⁻¹. The appearance of these bands is undoubtedly evidence that the crystal field in $K_6 C_{60}$ is stronger than that in the C_{60} crystal. This field intensification may be a consequence of charge transfer from potassium atoms to atoms of the C_{60} carbon molecules, as in the case of intercalated graphite.³⁴ Charge transfer in intercalated graphite is accompanied by a strengthening of the carbon-carbon bond.³⁴ It has been suggested⁷ that this strengthening may be responsible for the shift of the bands upon the doping of C_{60} . Comparing the spectra of C_{60} and $K_6 C_{60}$, we find the most noticeable low-frequency shifts for the following bands (Table II): 709 (C_{60}) → (655–675) ($K_6 C_{60}$), 772 → (726–760), 1250 → 1234, 1424 → 1386, 1468 → 1430, and 1574 → (1473–1480) cm⁻¹.

3.3. Mechanisms for resonant Raman scattering in C_{60}

When the Raman scattering of the C_{60} film is excited by the lines of the argon-krypton laser, the spectra are resonantly intensified, since the exciting light falls in an absorption region,¹⁰ although the band of the allowed electronic transition is at $\lambda < 350$ nm. In this case it is convenient to expand the Raman polarizability in a Taylor series in the internuclear coordinate in order to analyze the mechanisms for the resonant scattering.³⁵ The first two terms of this expansion determine the basic components of the Raman intensity. The first term corresponds to the Franck–Condon component,³³ and the second to the Herzberg–Teller interaction.³⁶

The Franck–Condon component is important only for completely symmetric vibrations (for the A_g vibrations in C_{60}). It increases dramatically as we approach an allowed electronic transition.³³ The Herzberg–Teller interaction becomes important when the exciting light falls in a weak electronic band near a strong electronic transition.³⁶ The Herzberg–Teller component differs from the Franck–Condon component in that it may determine the Raman intensity for both completely symmetric and asymmetric modes. To determine the possible Herzberg–Teller components of certain modes of C_{60} or others, we must resort to group theory.

For this analysis we make use of the circumstance that the intense absorption band in C_{60} corresponding to an al-

lowed electronic transition has the symmetry F_{1u} , while the weak bands in the visible region, which correspond to symmetry-forbidden transitions,¹⁵ can have a variety of symmetries.^{21,22} The only ones which are important for an analysis of the Herzberg–Teller component of the Raman scattering are odd representations (F_{2u} , G_u , and H_u), since only these representations can lead to even representations which are active in Raman scattering in direct products with F_{1u} . These products are

$$\begin{aligned} F_{1u} \otimes F_{2u} &= G_g + H_g, \\ F_{1u} \otimes G_u &= F_g + G_g + H_g, \\ F_{1u} \otimes H_u &= F_{1g} + F_{2g} + G_g + H_g. \end{aligned} \quad (3)$$

It can be seen from (3) that the expansion of direct representations has no completely symmetric representations A_g , but there are some Raman-active, quintuply degenerate H_g vibrations. In the Raman spectra of the C_{60} molecules, the major components of the Raman scattering (the Franck–Condon and Herzberg–Teller components) are thus separated in such a way that the Franck–Condon component is seen only in the completely symmetric A_g modes, and the Herzberg–Teller component only in the asymmetric H_g modes. With these thoughts in mind, we turn to the Raman spectra of the C_{60} film for the various excitation wavelengths (Fig. 2).

Among the completely symmetric vibrations in the C_{60} spectrum are the bands at 496 and 1468 cm⁻¹. While the intensity of the 1468-cm⁻¹ band increases substantially with decreasing λ_i , that of the 496-cm⁻¹ band remains essentially the same. The intensification of the 1468-cm⁻¹ band is determined exclusively by the Franck–Condon factor, which depends on the overlap of the vibrational wave functions in the ground and excited states. This overlap is at a maximum when the deformation of the molecule in its excited state follows the shape of this vibration. It can thus be concluded that the shapes of the normal vibrations at 1468 cm⁻¹ correspond closely to those changes in the internuclear distances in the C_{60} molecule which are manifested in the excited state.

Among the asymmetric H_g vibrations, those which intensify most noticeably with decreasing λ_i are the bands at 709, 1434, and 1574 cm⁻¹. Since the intensification of these modes is a consequence of the Herzberg–Teller interaction, it can be suggested that the changes in the potential energy are greatest (i.e., $\partial V / \partial R$ is a maximum) in the case of these vibrations. These changes in the potential energy determine the effectiveness of the Herzberg–Teller mechanism.

3.4. Resonant Raman scattering in the $K_6 C_{60}$ crystal

In the case of excitation at $\lambda_i = 1064$ nm, the intensities of the A_g bands at 500 and 1430 cm⁻¹ in the Raman spectra of $K_6 C_{60}$ are anomalously low (Fig. 3). In the case $\lambda_i = 647.1$ nm, in contrast, these bands are very intense; with $\lambda_i = 488$ nm they are of about the same intensity. We believe that this unusual behavior of the A_g bands stems from an interference of the partial scattering amplitudes determined by the components corresponding to each of the nearest electronic levels in the resultant amplitude for Raman scattering.³⁷ Our reasoning here is that an additional electronic level E_2 appears near 1.6 eV in the $K_6 C_{60}$ crys-

tal,²⁰ distinguishing this crystal from the C₆₀ crystal. The component corresponding to this electronic level may interfere with the component from the allowed intramolecular transition E₁ (at λ < 350 nm in C₆₀, the relation E₁ > E₂ holds). In this case the resultant amplitude for Raman scattering is, for the Franck–Condon component,

$$\alpha = \frac{\beta_1}{E_1 - \hbar\omega_i - i\Gamma_1} + \frac{\beta_2}{E_2 - \hbar\omega_i - i\Gamma_2}, \quad (4)$$

where the matrix elements β₁ and β₂ characterize the overlap of the vibrational wave functions. If β₁ and β₂ differ in sign, as they may in the case of the Franck–Condon mechanism for completely symmetric modes,³⁷ there may be a destructive interference of the components from the E₁ and E₂ levels under the condition ħω_i < E₂, and α will have extrema near E₁ and E₂. This behavior of α(ω_i) provides a qualitative explanation for the observed resonant profile of the excitation of Raman scattering for the completely symmetric modes in the K₆C₆₀ spectra. This behavior also explains why the A_g bands in K₆C₆₀ are much weaker than those in C₆₀ at an excitation wavelength λ_i = 1064 nm (Figs. 2 and 3).

In the Raman spectra of K₆C₆₀ we find that the intensities of doublets (267–280, 419–426, 655–675, 726–760, 1091–1118, and 1473–1480 cm⁻¹) vary with the excitation wavelength. These variations may be a consequence of the different symmetries of these components, since they appear as the result of a static splitting of the quintuply degenerate intramolecular H_g vibrations into doublets E_g + F_g in the crystal field of symmetry T_h for the local site of the C₆₀ molecule in the K₆C₆₀ crystal.

3.5. Second-order Raman scattering spectra in C₆₀ and K₆C₆₀ crystals

In the case of excitation with λ_i = 514.5 and 488 nm, the second-order Raman scattering spectra in C₆₀ and K₆C₆₀ are comparatively intense (in terms of peak intensity, they are weaker than the fundamental bands by a factor of only 10–50). The explanation apparently lies in the resonant nature of the spectra (Fig. 5). At λ_i = 1064 nm these spectra are very weak, because they are remote from electronic transitions. At λ_i = 647.1 nm they fall in the region of the triplet luminescence of C₆₀ and also in a region in which our spectrometer is relatively insensitive.

The bands in the second-order spectra are not broad. The reason is that the dispersion of the intramolecular modes is only slight.^{14,17,30} The peaks observed in the region 1500–3100 cm⁻¹ can thus easily be assigned to various sum and overtone combinations. Interestingly, all the sum and overtone combinations of the H_g modes which might fall in the frequency region of interest are seen in the spectra. This is a consequence of the sequential interaction of two Herzberg–Teller processes for each H_g mode in the given combination.

The overtones of the completely symmetric modes (2A_g) and also the sum combinations involving A_g modes (A_g + A_g and A_g + H_g) turn out to be weak. The reason may be that the Franck–Condon component of the intensity of the two-phonon scattering is very small. That the Franck–Condon component is negligible is also demonstrated by the absence of overtones of IR-active modes. It seems that the Franck–Condon component is slightly greater in the K₆C₆₀ spectra, in which combinations involving A_g modes can be seen more clearly. As we go from λ_i = 488 to 514.5 nm we

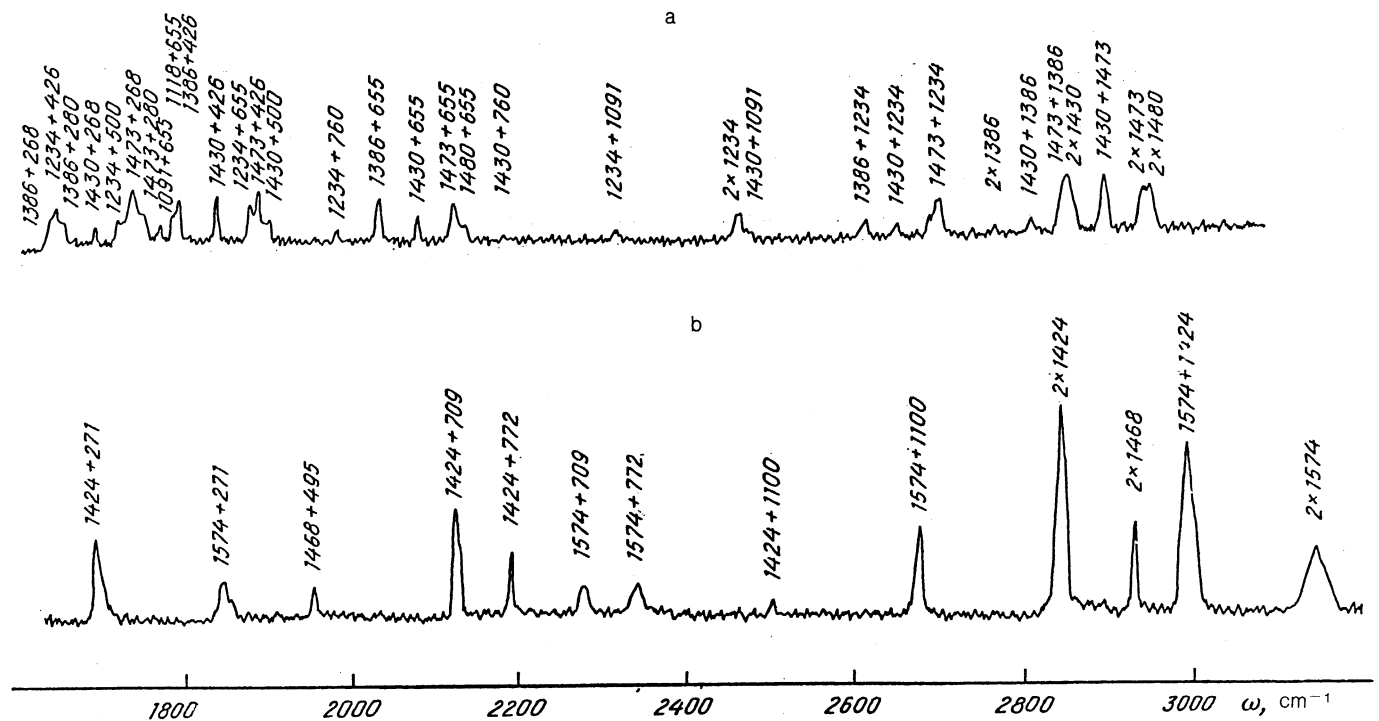


FIG. 5. Second-order Raman spectra of (a) K₆C₆₀ and (b) C₆₀ films, excited at λ_i = 488 nm.

see a tendency toward some increase in the intensities of these combinations. This increase agrees with the interference properties of the Raman intensities as discussed above. On the other hand, these intensities are slightly lower in the spectrum of C_{60} at $\lambda_i = 514.5$ nm, as we might expect for the Franck-Condon factor in the C_{60} crystal.

4. CONCLUSION

The vibrations of the C_{60} molecule and the C_{60} , K_3C_{60} , and K_6C_{60} crystals have been analyzed by group theory. It has been shown that the intermolecular vibrations (translational vibrations of potassium atoms and reorientations of C_{60} molecules) are not active in the Raman or IR absorption spectra of the C_{60} crystal, but they do become active in the K_3C_{60} and K_6C_{60} crystals. Some low-frequency bands observed in the Raman spectra of K_6C_{60} here for the first time have been attributed to translational motions of potassium atoms and to reorientations of C_{60} molecules. It has been found that the quintuply degenerate intramolecular H_g vibrations should split into doublets in the crystal field in all these crystals. This splitting, however, turns out to be very slight in the case of the C_{60} crystal, since the crystal field is weakened by the dynamic reorientation of molecules. In the spectra of K_6C_{60} we find a doublet splitting of the H_g bands, with a separation between the components ranging up to 34 cm^{-1} .

Analysis of the symmetry of the electronic states has revealed that the mechanisms for the Raman scattering are different for the A_g and H_g vibrations. While the intensity of the A_g bands is determined by the Franck-Condon component, that of the H_g bands depends on only the Herzberg-Teller interaction. This conclusion is supported by the second-order Raman spectra. The excitation profile of the Raman spectra for the A_g bands in the C_{60} crystal reveals that the expected changes in the internuclear distances in the excited state of the C_{60} molecule should be close in shape to the normal vibration at 1468 cm^{-1} of symmetry A_g . The anomalous behavior of the intensities of the A_g bands as a function of the excitation wavelength, on the one hand, and the very low intensity of the A_g modes at $\lambda_i = 1064$ nm in K_6C_{60} , on the other, are attributed to an interference of the contributions from the allowed electronic transition in the C_{60} molecule and the new electronic transition near 1.6 eV, which appears when C_{60} is doped with potassium atoms.

This work was supported by the Scientific Council on the Problem of High Temperature Superconductivity of the Russian Academy of Sciences, as part of Project 90575 (V. N. D. and B. N. M.), and by Progetti Finalizzati Scryctac

and Materiali Speciali per Technologie Avanzate of the Consiglio Nazionale della Ricerche (Italy).

- ¹ A. F. Hebard, M. J. Rosseinsky, R. C. Haddon *et al.*, *Nature* **350**, 600 (1991).
- ² K. Tanagaki, T. W. Ebessen, S. Saito *et al.*, *Nature* **352**, 222 (1991).
- ³ D. S. Bethune, G. Meijer, W. C. Tang *et al.*, *Chem. Phys. Lett.* **174**, 219 (1990).
- ⁴ R. C. Haddon, A. F. Hebard, M. J. Rosseinsky *et al.*, *Nature* **350**, 320 (1991).
- ⁵ D. S. Bethune, G. Meijer, W. C. Tang *et al.*, *Chem. Phys. Lett.* **179**, 181 (1991).
- ⁶ K.-A. Wang, Y. Wang, P. Zhou *et al.*, *Phys. Rev. Lett.*, 1992 (in press).
- ⁷ S. J. Duclos, R. C. Haddon, S. H. Glarum *et al.*, *Solid State Commun.*, 1992 (in press).
- ⁸ R. Danieli, V. Denisov, G. Ruani *et al.*, *Solid State Commun.*, 1992 (in press).
- ⁹ W. Kraetschmer, K. Fostiropoulos, and D. R. Huffman, *Chem. Phys. Lett.* **170**, 167 (1990).
- ¹⁰ W. Kraetschmer, L. D. Lamb, K. Fostiropoulos *et al.*, *Nature* **347**, 354 (1990).
- ¹¹ J. P. Hare, T. J. Dennis, H. W. Kroto *et al.*, *J. Chem. Soc. Chem. Commun.*, 412 (1991).
- ¹² C. I. Frum, R. Engleman, H. G. Hedderick *et al.*, *Chem. Phys. Lett.* **176**, 504 (1991).
- ¹³ K. Aoki, H. Yamawaki, Y. Kakudate *et al.*, *J. Phys. Chem.* **95**, 9037 (1991).
- ¹⁴ R. L. Cappelletti, J. R. D. Copley, W. A. Kamitakahara *et al.*, *Phys. Rev. Lett.* **66**, 3261 (1991).
- ¹⁵ J. W. Arbogast, A. P. Darmany, C. S. Foote *et al.*, *J. Phys. Chem.* **95**, 11 (1991).
- ¹⁶ M. Terazima, N. Hirota, H. Shinohara *et al.*, *J. Phys. Chem.* **95**, 9080 (1991).
- ¹⁷ K. Prassides, J. Tomkinson, C. Christides *et al.*, *Nature* **354**, 462 (1991).
- ¹⁸ O. V. Dolgov and I. I. Mazin, *Solid State Commun.*, 1992 (in press).
- ¹⁹ C. Varma, J. Zaanen, K. Raghavachari *et al.*, *Science* **254**, 989 (1991).
- ²⁰ P. J. Benning, J. L. Martins, J. H. Weaver *et al.*, *Science* **252**, 1417 (1991).
- ²¹ S. Larsson, A. Volosov, A. Rosen *et al.*, *Chem. Phys. Lett.* **137**, 1501 (1987).
- ²² F. Negri, G. Orlandi, F. Zerbetto *et al.*, *Chem. Phys. Lett.* **144**, 31 (1989).
- ²³ S. H. Yang, C. L. Pettiette, J. Conceicao *et al.*, *Chem. Phys. Lett.* **139**, 233 (1987).
- ²⁴ P. W. Stephens, L. Mihaly, P. L. Lee *et al.*, *Nature* **351**, 632 (1991).
- ²⁵ O. Zhou, J. E. Fisher, N. Coustel *et al.*, *Nature* **351**, 462 (1991).
- ²⁶ R. Tycko, R. C. Hadden, G. Dabagh *et al.*, *J. Phys. Chem.* **95**, 518 (1991).
- ²⁷ R. Tycko, G. Dabagh, R. M. Fleming *et al.*, *Phys. Rev. Lett.* **67**, 1886 (1991).
- ²⁸ P. A. Heiney, J. E. Fisher, A. R. McGhie *et al.*, *Phys. Rev. Lett.* **66**, 2911 (1991).
- ²⁹ B. N. Mavrin, *Opt. Spectrosc.* **49**, 79 (1980).
- ³⁰ D. E. Weeks and W. G. Harter, *J. Chem. Phys.* **90**, 4744 (1989).
- ³¹ A. F. Goncharov, V. N. Denisov, B. N. Mavrin *et al.*, *Zh. Eksp. Teor. Fiz.* **94**(11), 321 (1988) [*Sov. Phys. JETP* **67**(11), 2356 (1988)].
- ³² M. M. Sushinskiĭ, *Raman Spectra of Molecules and Crystals* [in Russian], Nauka, Moscow, 1969, Section 21.
- ³³ D. L. Rousseau and P. F. Williams, *J. Chem. Phys.* **64**, 3519 (1976).
- ³⁴ C. T. Chan, K. M. Ho, and W. A. Kamitakahara, *Phys. Rev. B* **36**, 3499 (1977).
- ³⁵ A. C. Albrecht, *J. Chem. Phys.* **34**, 1476 (1961).
- ³⁶ J. M. Friedman and R. M. Hochstrasser, *Chem. Phys.* **1**, 457 (1973).
- ³⁷ J. M. Friedman and R. M. Hochstrasser, *Chem. Phys. Lett.* **32**, 414 (1975).

Translated by D. Parsons